Wind and Structures, *Vol. 27, No. 3 (2018) 187-197*
DOI: https://doi.org/10.12989/was.2018.27.3.187

Analysis of aerodynamic characteristics of 2 MW horizontal axis large wind turbine

Akin Ilhan[1a], Mehmet Bilgili[*2] and Besir Sahin[1b]

[1]*Department of Mechanical Engineering, Faculty of Engineering, Cukurova University, 01330 Adana, Turkey*
[2]*Department of Mechanical Engineering, Faculty of Ceyhan Engineering, Cukurova University, 01950 Adana, Turkey*

(Received September 28, 2017, Revised January 14, 2018, Accepted January 19, 2018)

Abstract. In this study, aerodynamic characteristics of a horizontal axis wind turbine (HAWT) were evaluated and discussed in terms of measured data in existing onshore wind farm. Five wind turbines (T1, T2, T3, T4 and T5) were selected, and hub-height wind speed, U_D, wind turbine power output, P and turbine rotational speed, Ω data measured from these turbines were used for evaluation. In order to obtain characteristics of axial flow induction factor, a, power coefficient, C_p, thrust force coefficient, C_T, thrust force, T and tangential flow induction factor, a', Blade Element Momentum (BEM) theory was used. According to the results obtained, during a year, probability density of turbines at a rotational speed of 16.1 rpm was determined as approximately 45%. Optimum tip speed ratio was calculated to be 7.12 for most efficient wind turbine. Maximum C_p was found to be 30% corresponding to this tip speed ratio.

Keywords: aerodynamic problem; structural dynamic analysis; wind energy; wind loads; wind velocity; wind-structure interaction

1. Introduction

Greenhouse gas emissions being a global threat in global warming seem to be doubled by the year of 2050. An increased demand on the fossil oil seems to enlarge the related concerns on the preservation of environment. In this respect, a high rate of progress in energy systems is vitally needed to take effective role in achieving a 50% reduction of CO_2 emissions relative to current levels by 2050 globally (Bilgili *et al.* 2015). Energy efficiency, energy storage, nuclear energy and CO_2 capture and storage play an important role in the context of this energy progress. Additionally, renewable energy is one of the most important energy sources in addressing the global energy and environmental challenges. However, amongst renewable energy sources, wind power is the fastest growing sector for electricity generation for the past years (Ohunakin and Akinnawonu 2012, Rodriguez-Hernandez *et al.* 2016). Also, for some developed countries, energy share obtained from wind comprises 15% to 30% of the total electricity generations. Fig. 1 presents the cumulative wind power installed capacity for the World and European Union from 2000 to 2016. Currently, the installed wind power capacities are 486.8 GW and 153.7 GW for the World and European Union, respectively.

A functional relation is valid during the interaction of the rotor of a turbine and wind in terms of power generation, i.e. the aerodynamic forces are generated within this concept. Wind shear and off-axis winds cause a periodic aerodynamic forces and fluctuating forces occurring arbitrarily which are induced by turbulence and dynamic effects (Manwell *et al.* 2009). In this sense, aerodynamic performance of a wind turbine of a certain region is needed to be well understood since aerodynamics has become a vital factor in the evaluation of turbine system design. Thus, it requires enough knowledge by means of average wind conditions, as well wind turbulence and wind events of extreme conditions to meet the necessities of aerodynamic performance. This information can be appraised during the design and selection of a wind turbine for a considered region of interest. Performance analysis is needed to be conducted to reveal the energy productivity and cost effectiveness of a certain wind energy system. Optimum wind speed status is important in loading management and constitution of operational procedures. Thus, related information are used for defining of operational factors, start-up and shutdown functions, lifetime of the systems, and also requirements related with the maintenances and operations (Kishinami *et al*. 2005, He *et al.* 2013).

In recent years, many works on wind characteristics and aerodynamic characteristics of horizontal axis wind turbines (HAWTs) have been performed (Ashrafi *et al*. 2015). As an effective tool, the classical blade element momentum (BEM) theory and the modified BEM as well as computational fluid dynamics (CFD) and the BEM-CFD mixed approach have been frequently used to develop mathematical laws for design and optimization purposes of these kind of wind turbines (Bai and Wang 2016). Hansen *et al.* (2006) have gathered a comprehensive review of aerodynamic theories and aeroelasticity devoted to the wind turbine designs. Cao *et al.* (2009) investigated the wind characteristics of a strong typhoon using the wind speeds measured

∗Corresponding author, Professor
E-mail: mbilgili@cu.edu.tr
[a] Ph.D. Student
[b] Professor

ISSN: 1226-6116 (Print), 1598-6225 (Online)

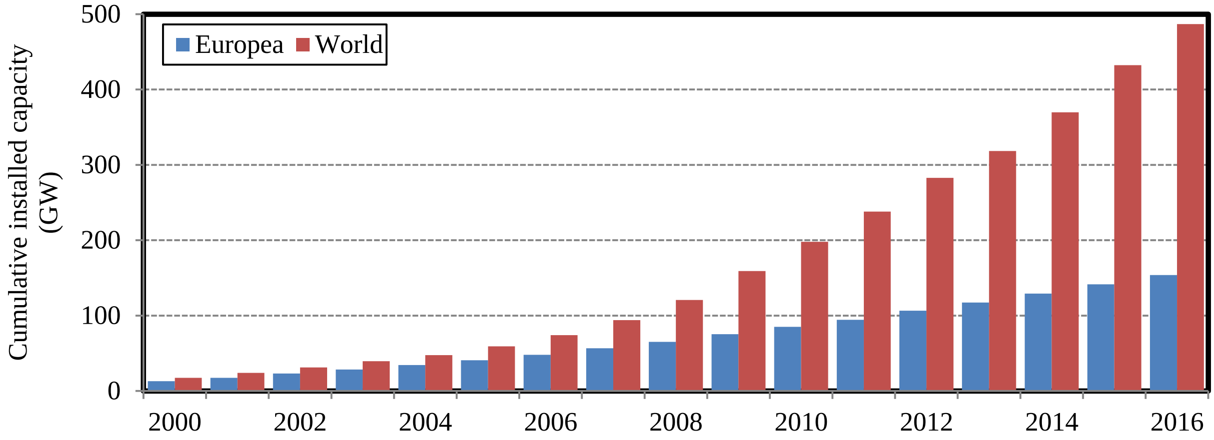

Fig. 1 Comparison of cumulative installed capacity of wind power between Europe and the World

simultaneously by nine vane and seven sonic anemometers at a height of about 15 m from the ground level. In their study, various wind characteristics such as turbulence intensity and scale, gust factor, peak factor, decay factor of the coherence function, probability distribution function, power spectrum, and their variations with wind speed were obtained. Using the BEM theory, Tenguria *et al.* (2010) investigated the performance of wind turbine blade for a 5 KW HAWT.

Lanzafame and Messina (2010) investigated the influence of rotor rotational velocity on horizontal axis wind turbine performance using the BEM theory. They also produced a methodology which allows a HAWT to work continuously at its maximum power coefficient. Using the BEM theory, Bavanish and Thyagarajan (2013) presented the effect of power coefficient for different blade angle, tip speed ratio, ratio of coefficient of drag and coefficient of lift and blade solidity. Based on the BEM theory, Sedaghat *et al.* (2014) introduced a new quadratic formulation for the angular induction factor which incorporated all important design parameters including drag to lift ratio, axial induction factor, and the local speed ratio. They have also proposed that the present extended BEM method may also be useful in enhancing robustness and convergence speed of iterative numerical schemes used widely in conventional wind turbines. Ashrafi *et al*. (2015) designed a 200 kW HAWT blade using an efficient iterative algorithm based on the BEM theory on aerodynamic of wind turbines. They also investigated the effects of off-design variations of wind speed on the blade performance parameters according to constant rotational speed of the rotor.

Jeon *et al*. (2015) investigated the wind turbines affected by the wake of neighboring wind turbines, which reduces power production and shortens turbine life due to the mechanical fatigue. They also compared the wake models using the values measured from a commercially operated onshore wind farm. Karthikeyan *et al.* (2015) made a comprehensive review of aerodynamic developments on the small HAWT blade. Wekesa *et al.* (2016) presented empirical and computational approaches to investigate aerodynamic performance of the small wind turbine in operation at arid rural Mwingi-Kitui plateau region, Kenya.

In order to improve the BEM theory, Sun *et al*. (2016) derived two new BEM methods with Glauert’s tip correction and Shen’s tip correction. They also highlight that the improved BEM theory gives a better prediction than the classic BEM method, especially in the blade tip region. Bai and Wang (2016) made a comprehensive review of computational and experimental approaches to analysis of aerodynamic performance in HAWTs.

Wang *et al.* (2016) analyzed non-stationary wind characteristics using the wind data recorded by the Structural Health Monitoring System (SHMS) of the Sutong Bridge (Jiangsu Province, China) in Typhoon Damrey. The wind characteristics such as the mean wind speed, turbulence intensity, gust factor and power spectral density were discussed and compared. Ageze *et al*. (2017) made an overview for the aeroelastic tool of wind turbines. This overview indicates the previous efforts made on wind power technology, unresolved issues, and future directions of wind power generation technology. Khanjari *et al.* (2017) presented the analysis of energy and exergy of a horizontal axis wind turbine based on the BEM theory. Their results show that the BEM theory has an effective ability to predict the energy and exergy efficiencies of the wind turbines. Tao *et al.* (2017) made the stationary and nonstationary analysis of the wind characteristics of a strong wind event from a landfall typhoon recorded at Sutong Bridge site (Jiangsu Province, China). In their study, the wind characteristics such as the mean wind speed, turbulence intensity, gust factor, peak factor, and turbulence integral scale as well as turbulence power spectral density and evolutionary power were comprehensively analyzed based on the traditional stationary model and the two recent nonstationary models. Pinto and Gonçalves (2017) presented a revised theoretical analysis of aerodynamic optimization of HAWTs, including drag effects, based on the BEM theory.

Full-scale wind characteristics based on the field measurements is essential to accurately modeling wind effects on structures (Zidong *et al.* 2017). Fundamental aerodynamic parameters can shortly be introduced to involve of an actual power extracted by turbine, P, axial flow induction factor, a, power coefficient, C_p, thrust force coefficient, C_T, thrust force on the air, T, tip speed ratio, λ

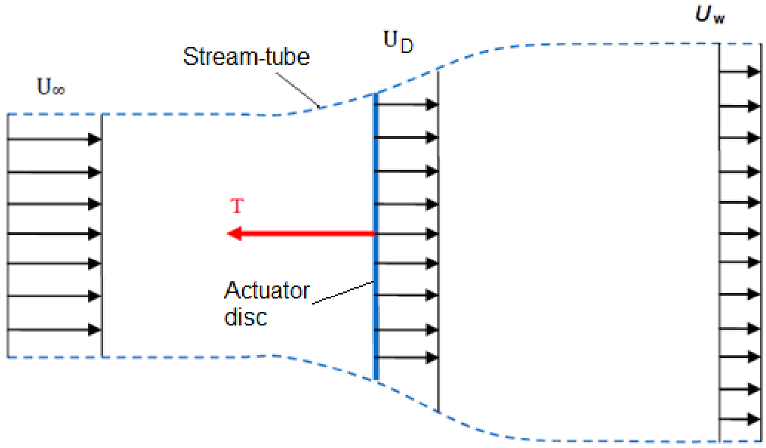

Fig. 2 Schematic representation of the actuator disc model of a wind turbine and stream tube

and finally tangential flow induction factor, *a'* (Wekesa *et al.* 2016, Hansen *et al.* 2006, Sedaghat *et al.* 2014, Lanzafame and Messina 2010, Ashrafi *et al.* 2015). The behavior of these aerodynamic parameters dependent on free-stream wind speed, U_∞, rotational speed, Ω and rotor radius, *R* is substantially important in enhancing the quality of the technological developments. In additions, wind turbine aerodynamic characteristics are inevitably necessary tools for performance monitoring, turbine controlling and power forecasting. In the present study, aerodynamic characteristics of a HAWT including *P, a*, C_P, C_T, *T* and *a'* parameters were analyzed as a function of λ using industrial data such as hub-height wind speed, U_D, turbine rotational speed, Ω and turbine power output, *P* measured from the operating wind power plant.

2. Material and method

Fig. 2 presents the actuator disc model of a wind turbine. The blade element momentum (BEM) theory, as the most common wind turbine analysis method, is used in this study. The BEM theory can be divided into two parts. In the first part, the conservation of linear momentum is applied to the control volume enclosing the whole system. The turbine rotor is modeled as an actuator disc in a one dimensional stream tube. In this model, the actuator disc is responsible for wind speed reduction as the flow passed over the disc, and it is assumed that no rotation is imparted to the flow (Ashrafi *et al.* 2015). Furthermore, useful mechanical energy that is captured by the conversion from kinetic energy of wind depends on the optimum wind turbine airfoil design. The surface and two cross-sections of the stream tube are given as the boundaries of the control volume in the analysis of considered control volume. Uniform “actuator disc” represents the turbine and creates a pressure discontinuity on the air flowing through the stream tube. In the second part, considering the rotating annular stream tube, the angular momentum theory, which is related to rotor torque, is applied. In the case of a rotating wind turbine rotor, the flow behind the rotor rotates in the opposite direction to the rotor, in reaction to the torque exerted by the flow on the rotor (Manwell *et al.* 2009).

Analysis for aerodynamic relations of horizontal axis wind turbines is not limited to any special turbine type. Ideal flow conditions are considered for this analysis (Mathew 2006). Thus, this analysis involves the assumptions stated below as defined by Burton *et al.* (2011): 1) Fluid flow properties involve homogenous, incompressible, and steady state conditions; 2) Frictional drag is assumed not to be given; 3) Number of blades is assumed as infinite due to consideration of the rotating annular stream tube for the turbine rotor; 4) Uniform assumption of thrust over the disc or rotor area is taken into consideration; 5) Non-rotating fluid conditions are given at the down-stream wake; 6) The static pressure is assumed to be set equal to the undisturbed ambient static pressure at locations of far upstream and far downstream of the rotor. Some of these assumptions may be questionable when we consider the real flow conditions around a wind turbine. For example, the practical rotor has finite number of blades and the aerodynamic drag and tip losses cannot be neglected. In additions, the flow ahead and behind the rotor is not completely axial as assumed under the ideal condition. When the fluid applies torque to the rotor, as a reaction, rotational wake is generated downstream of the rotor. These will cause energy loss and reduce the peak power coefficient (Mathew 2006).

There is an enlargement in cross-sectional area of stream tube in axial direction initially smallest in far upstream and largest in far downstream. In terms of aerodynamic conservation principle, considering steady state flow case, Eqs. (1) and (2) are set as follows

$$\dot{m}_{in} = \dot{m}_{out} \tag{1}$$

$$\rho A_\infty U_\infty = \rho A_D U_D = \rho A_w U_w \tag{2}$$

While denotations of *ρ* for density, *A* for cross-sectional area and *U* for flow velocity are used in equations; subscripts of “∞”, “*D*” and “*W*” symbols refer to far upstream, disc and far wake conditions respectively.

Induction of velocity variation by the actuator disc that is superimposed on the free-stream velocity, U_∞ is shown by Eq. (3) where U_D stands for net stream-wise velocity (Burton *et al*. 2011)

$$U_D = U_\infty (1 - a) \tag{3}$$

Velocity at far fake, U_w dependent on the free-stream velocity, U_∞ and the velocity induction factor, a superimposed on the free-stream velocity, U_∞ is given by Eq. (4).

$$U_w = U_\infty (1 - 2a) \tag{4}$$

Considering Eqs. (3) and (4) and axial flow induction factor, a, the thrust force, T and power output, P can be determined as

$$T = 2\rho A_D U_\infty^2 a(1-a) \tag{5}$$

$$P = 2\rho A_D U_\infty^3 a(1-a)^2 \tag{6}$$

General form of power coefficient, C_p and its simplified form are defined with Eqs. (7) and (8), respectively

$$C_p = \frac{P}{\frac{1}{2}\rho U_\infty^3 A_D} \tag{7}$$

$$C_p = 4a(1-a)^2 \tag{8}$$

Eq. (9) indicates the derivation of power coefficient, C_p with flow induction factor, a to determine the maximum value of power coefficient, C_{pmax} for a=1/3

$$\frac{dC_p}{da} = 4(1-a)(1-3a) = 0\ ; C_{p\max} = 16/27 = 0.593 \tag{9}$$

It is known that the Betz limit is defined for the maximum achievable value of the power coefficient, C_p that cannot be exceeded in bare wind turbines (Burton et al. 2011). Beyond the power coefficient, C_P, the thrust coefficient, C_T is also used to non-dimensionally show the pressure drop formed by the force on the actuator disc as presented in Eq. (10). Simplified form of Eq. (10) gives thrust coefficient, C_T depending on simply flow induction factor, a given in Eq. (11).

$$C_T = \frac{T}{\frac{1}{2}\rho U_\infty^2 A_D} \tag{10}$$

$$C_T = 4a(1-a) \tag{11}$$

Torque that arises on the rotary disc will be equivalent to the ratio of the exchange of angular momentum caused by the passage of air through the disc.

$$\delta Q = \rho \delta A_d U_\infty (1-a) 2\Omega a' r^2 \tag{12}$$

Here, a' stands for the tangential flow induction factor, and r is the radius of the rotor disc. Rotor shaft power, P originating from the rotor disc is calculated using Eqs. (13) and (14).

$$\delta P = \delta Q \Omega \tag{13}$$

$$\delta P = \rho \delta A_d U_\infty (1-a) 2\Omega^2 a' r^2 \tag{14}$$

Eqs. (6) and (14) are considered together in order to obtain Eq. (15).

$$U_\infty^2 a(1-a) = \Omega^2 a' r^2 \tag{15}$$

At the edge of rotary disc, radius "r" is equal to the value of R. The blade local speed ratio, λ_r and blade tip speed ratio, λ are defined by Eqs. (16) and (17), respectively.

$$\lambda_r = \frac{r\Omega}{U_\infty} \tag{16}$$

$$\lambda = \frac{R\Omega}{U_\infty} \tag{17}$$

3. Results and discussion

The data used for the present study was provided from the Sebenoba Wind Energy Power Plant (WEPP), as presented in Fig. 3. By the year of 2008, this WEPP was put into operation including 17 identical wind turbines and the rated capacity of each turbine was 2 MW. The hub-height of the identical wind turbines is 67 m, and rotor diameter corresponds to 80 m. Consequently, total swept area of a single wind turbine is approximately 5027 m^2. Technical specifications of the identical turbines are provided in Table 1. The wind turbines operate with wind speeds within the range of 4 m/s≤U_∞≤25 m/s and nominal speed of the turbines corresponds to 15 m/s. Wind turbines are the pitch regulated upwind turbines with an active yaw and a three-bladed rotor.

Selected wind turbines symbolized as T1, T2, T3, T4 and T5 were used to evaluate the performance of turbines using parameters such as power output, P, hub-height wind speed, U_D and rotational speed, Ω. The existing data belongs to the whole year of 2013 with measurements taken in period of 10 minutes. Initially, 52560 (365 x 24 x 6) original data of U_D, Ω and P were categorized into a suitable number of classes. For the probability distribution of rotational speed, Ω; class limits were determined as 1.00-2.99, 3.00-4.99, 5.00-6.99, 7.00-8.99, 9.00-10.99, 11.00-12.99, 13.00-14.99 and 15.00-16.99 rpm. Average value in terms of rotational speed, Ω considering five

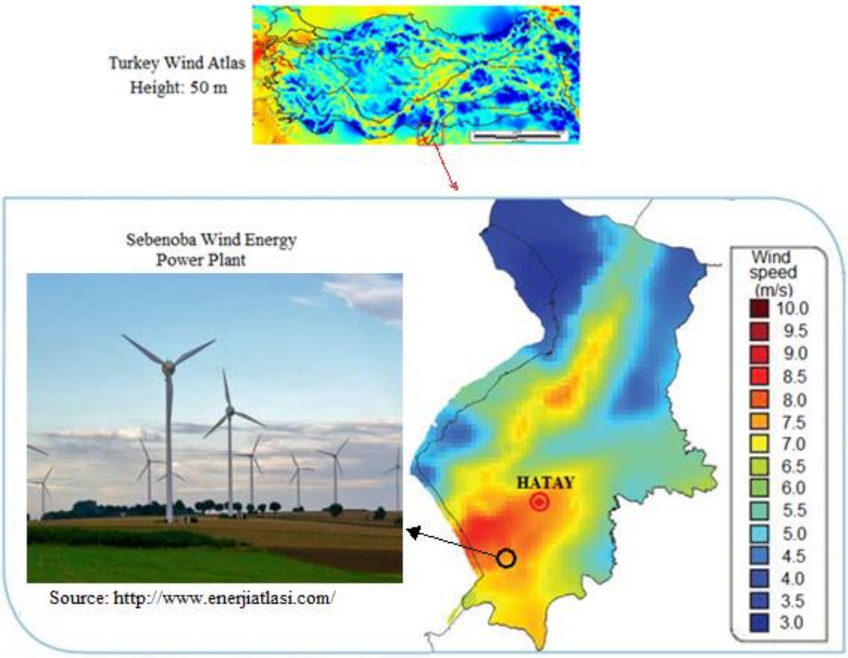

Fig. 3 Sebenoba wind energy power plant in Hatay province (REGD, 2017)

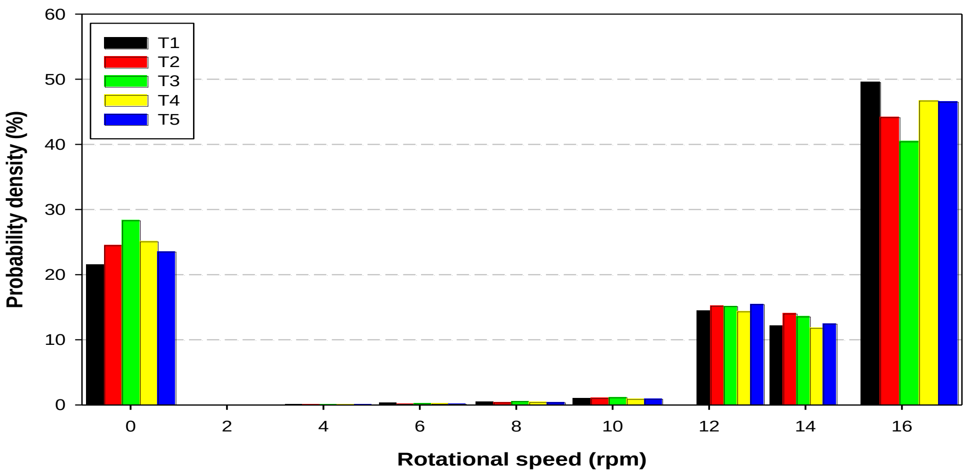

Fig. 4 Probability density of rotational speed, Ω

turbines taking the average observation values of each turbine into account was computed. In this way, considering all turbines, average values of observations for all classes were calculated to be 2.02, 4.10, 6.05, 8.08, 10.10, 12.44, 13.94 and 16.14 rpm as a function of rotational speed, Ω. Since, average values of observations contain multi-data, a secondarily operation is performed for all turbines where parameters such as U_D and P are defined with respect to the average observation values of rotational speed, Ω.

The probability density of rotational speed over a year is presented in Fig. 4. As seen from the figure, the rotational probability of wind turbines at the rotational speed of 0 rpm is approximately 22%. This data was probably formed for the cases of no wind case or sudden change of rotor position because of rapid alterations in wind speed, vortices forcing to change the position of the rotor, and these results may be obtained due to the breakdowns or maintenance of the wind turbines. In additions, for certain reasons such as maintenance and cut-out wind speed (beyond 25 m/s) no electric energy production can happen. On the other hand, the rotation probability of the turbine over a year is approximately 45% having a rotational speed of 16.11 rpm, at which the wind turbine has a nominal power production. Furthermore, all wind turbines operate at a nominal and close to nominal rotational speeds, Ω over half of the year. But, the rotation probability of wind turbines is very low (2%) at rotational speeds, Ω between 2.07 rpm and 10 rpm over a year.

Fig. 5 reveals variation of extracted power, P depending on the hub-height wind speed, U_D for different rotational speeds, Ω for turbine T1. It is also clear from this figure that enhancement of power, *P* can generally be achieved by the increase of hub-height wind speed, U_D or rotational speed, Ω. However, in terms of power, *P* and hub-height speed, U_D depending on a constant rotational speed, Ω, it is observed that this increase of power, *P* is seen only up to a certain value of hub-height wind speed, U_D. Rapid increase of power, *P* with respect to the hub-height wind speed, U_D is more apparent in the case of the optimum rotational speed, Ω.

It is not possible to have the optimum wind power characteristic curve as desired continuously due to wind gusts as seen in Fig. 5. Sudden and continuous fluctuations of wind speeds vary between 30% and 50% above or below the average of wind speeds due to the wind gusts. Complex wind structure and gusty wind rapidly alters the wind direction and magnitude of the wind speed causing a large scale vortices which avoids wind turbines to have optimum wind power generation as seen from Fig. 5.

Table 1 Technical properties of wind turbines (VESTAS 2017)

Equipment	Properties
Rotor	
Diameter	80 m
Area swept	5027 m^2
Nominal revolutions	16.7 rpm
Operational interval	9-19 rpm
Number of blades	3
Power regulation	Pitch/OptiSpeed
Air brake	Full blade pitch by three separate hydraulic pitch cylinders
Tower	
Hub height	67 m
Operational data	
Cut-in wind speed	4 m/s
Nominal wind speed	15 m/s
Cut-out wind speed	25 m/s
Generator	
Type	Asynchronous with OptiSpeed
Rated output	2000 kW
Operational data	50 Hz, 690 V
Gearbox	
Type	Planet / parallel axles
Control	
Type	Microprocessor-based control of all the turbine functions with the option of remote monitoring. Output regulation and optimization via OptiSpeed and OptiTip pitch regulation

Consequently, the resultant power output, *P* of wind turbines are mostly affected by gusty wind characteristics, the incoming wind direction and terrain roughness characteristics (Emejeamara *et al.* 2015). In the consideration of the effectiveness of the wind speed, and direction on the wind turbine performances; the topographic conditions must also be taken into account. Namely, orographic elements exert an additional influence on the characteristics of wind. For example, having rotational speed, Ω of 16.40 rpm, the power curve is well defined as the function of hub-height wind speed, U_D. But, having rotational speed in the range of 1.82 rpm$\leq\Omega\leq$13.95 rpm for turbine T1 cannot exactly match with the optimized power characteristic curve obtained at a nominal rotational speed of 16.40 rpm. But, they will be designed to mimic this curve near the target range of wind speeds as discussed elsewhere. As mentioned before, maximum power output rate of wind turbines over a year is approximately 45% under an optimum rotational speed. But, in the case of rotational speed, Ω ranging from 12.43 rpm to 13.95 rpm, power generation rate occurs at around 30% over a year. Although, there are occasionally high values of hub-height wind speed, U_D varying between 15 m/s and 25 m/s which corresponds to the rotational speeds, Ω in the range of 1.82 rpm$\leq\Omega\leq$ 16.4 rpm a wind power generation rate is very low and fluctuated as seen Fig. 5. These rotational speed variations happen due to the complexity of wind. That is to say, it is known that in the atmosphere, catastrophic large scale vortices are developed. These vortices alter the direction of wind speed frequently. Because of these reasons, it is not possible for wind turbines to follow the flow direction using yaw mechanism in short period of time. Namely, there is a phase shift between change of flow direction and yaw mechanism of the wind turbine.

Distributions of wind power, *P*, axial flow induction factor, *a*, power coefficient, C_P, thrust coefficient, C_T, thrust force, T and tangential flow induction factor, a' based on the dimensionless tip speed ratio, λ at an optimum rotational speed (16.4 rpm) are presented in Figs. 6-11. Generally, variation of wind power, *P* against tip speed ratio, λ reveals that power extracted from a wind turbine is inversely related with tip speed ratio, λ. Eq. (17) demonstrates that an increase of free-stream wind speed, U_∞ adversely affects the tip speed ratio, λ. It is also valid from Eq. (6) that free-stream wind speed, U_∞ positively affects the extracted power increase. Thus, under constant rotational speed, Ω, power, *P* and tip speed ratio, λ are inversely altered. Regarding this information, for the average of tip speed ratio, 2.90 of five turbines corresponds to the average power extraction, *P* of 2000 kW as seen in Fig. 6. According to the average data of five turbines, power generation rate doesn't change much for the range of tip speed ratio of 3.2$\leq\lambda\leq$5.12. On the other hand, power generation rate decreases rapidly for average tip speed ratio of λ>5.12. The power extracted at this average tip speed, λ value of 5.12 corresponds to power extraction of P=1781.41 kW as an average value of five turbines. Power generation results of turbines are in a good agreement for the whole range of tip speed ratio as seen in Fig. 6. It is observed from the data of five turbines,

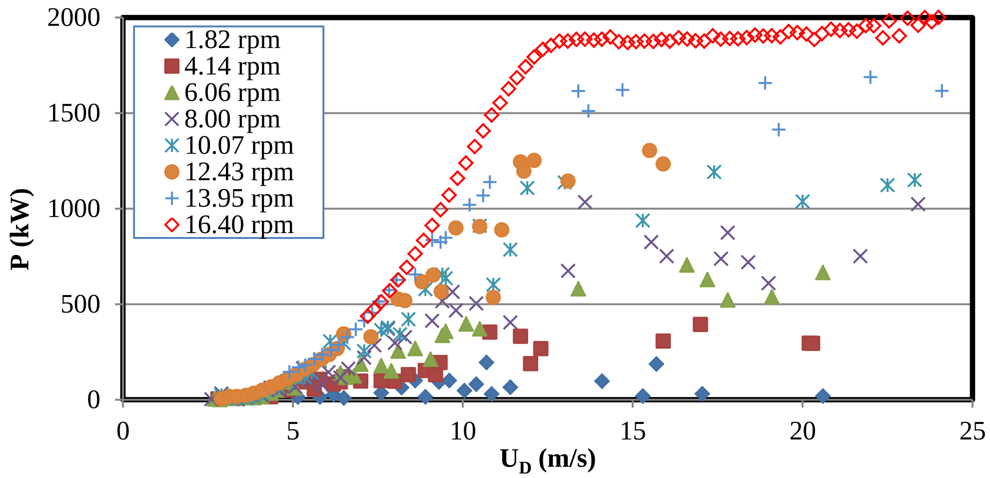

Fig. 5 Variation of power, P with hub-height wind speed, U_D at varied rotational speeds, Ω considering T1

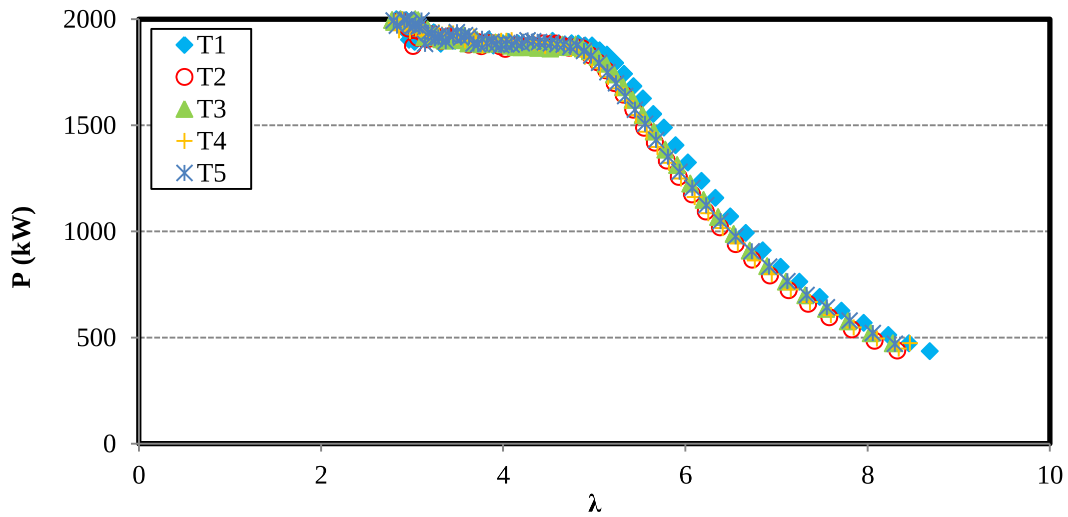

Fig. 6 Variation of power, P with tip speed ratio, λ for five turbines

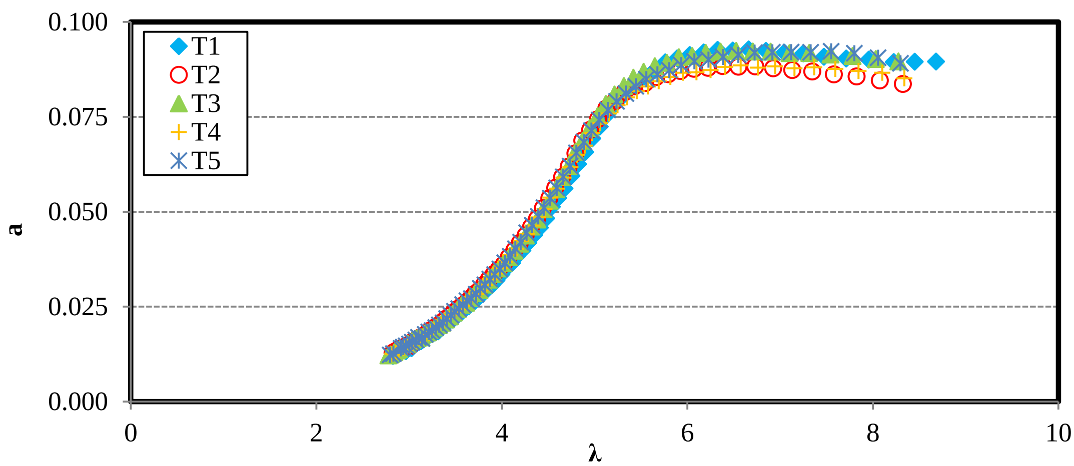

Fig. 7 Variation of flow induction factor, a with tip speed ratio, λ for five turbines

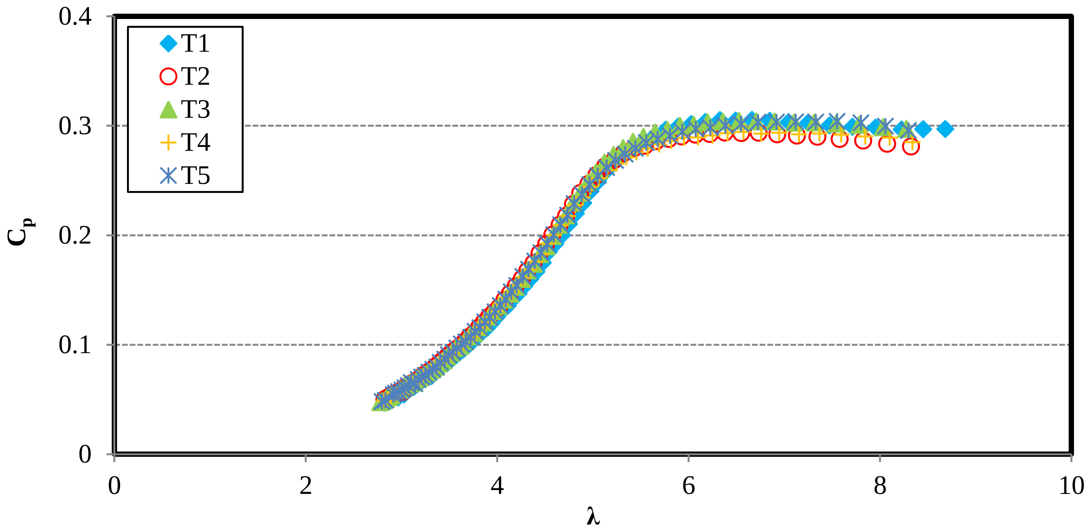

Fig. 8 Variation of power coefficient, C_p with tip speed ratio, λ for five turbines

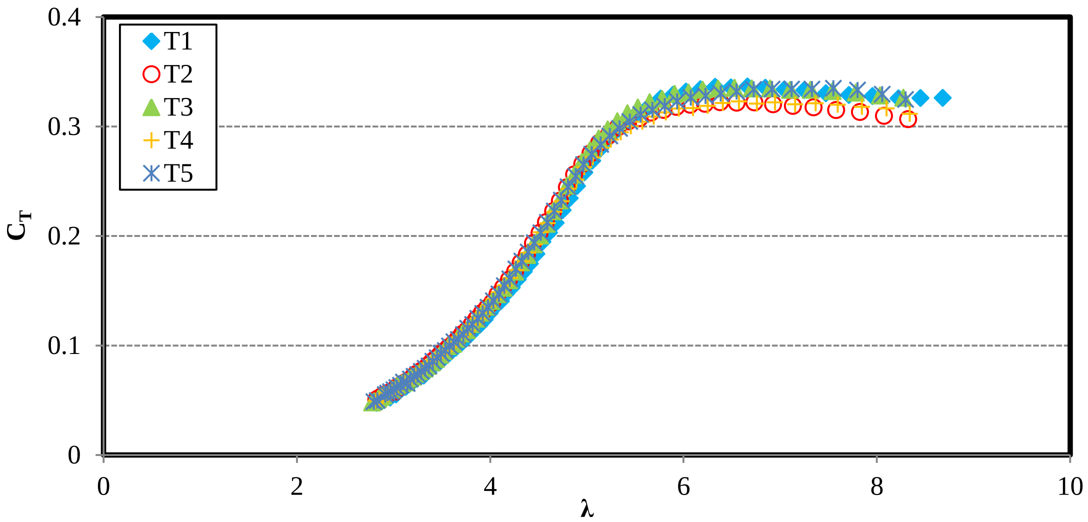

Fig. 9 Variation of thrust coefficient, C_T with tip speed ratio, λ for five turbines

the tip speed value of λ=5.12 is the critical value for variation of the power extraction which is altered from a lower slope of curve to a higher slope of curve.

Variation of flow induction factor, *a* depending on the tip speed ratio, λ for five turbines is shown in Fig. 7. Considering the average data of five turbines, a rapid increase of flow induction factor, *a* is observed for the tip speed ratio of 2.81≤λ≤6.10. Here, the range of average flow induction factor, *a* was determined to be 0.0124≤a≤0.0894. Considering this average range of tip speed ratio λ, for example, λ=2.81 free-stream wind speed, U_∞ and disc wind speed, U_D are 24.07 m/s and 23.77 m/s respectively. But, U_∞ and U_D are 11.10 m/s and 10.11 m/s respectively for the tip speed ratio λ=6.10.

Variation of power coefficient, C_p depending on the tip speed ratio, λ is presented in Fig. 8. An increase of power coefficient, C_p is observed at lower free-stream wind speeds, U_∞ corresponding to higher values of λ. According to the average data of five turbines, a rapid increase of power coefficient, C_p is valid for the average range of tip speed ratio of 2.81≤λ≤6.04. The power coefficient, C_p is computed to be $0.0482 \leq C_p \leq 0.2961$ for 2.81≤λ≤6.04. Thus, power coefficients, C_P of turbines are agreed well. In summary, a higher power coefficient values, C_p are obtained at lower free-stream wind speeds, U_∞ whereas, lower power coefficient values, C_P are obtained at a higher free-stream wind speeds, U_∞ in this range of tip speed ratio, λ. Considering the average data of five turbines, maximum power coefficient, C_p was computed as 30.03% at the tip speed ratio of λ=7.12.

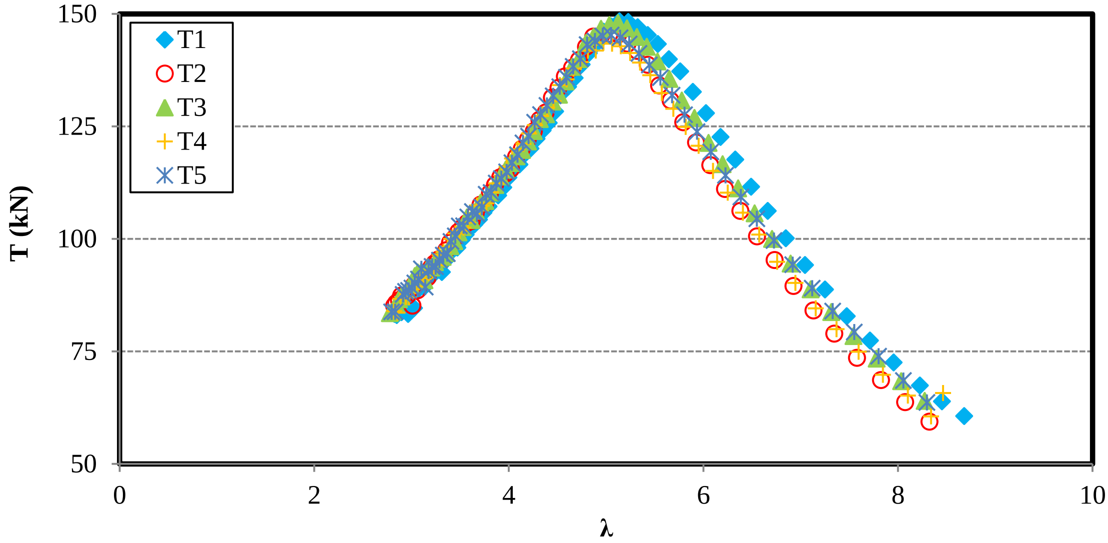

Fig. 10 Variation of thrust force, T with tip speed ratio, λ for five turbines

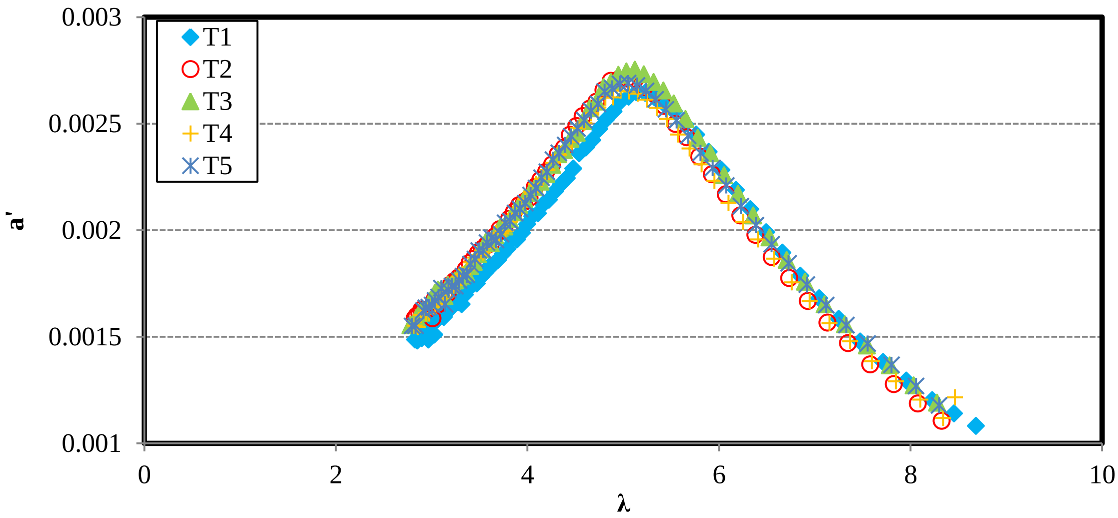

Fig. 11 Variation of tangential flow induction factor, a' with tip speed ratio, λ for five turbines

Considering data of five wind turbines, variation of thrust force coefficient, C_T depending on the tip speed ratio, λ is shown in Fig. 9. In the range of tip speed ratio of $2.81 \le \lambda \le 5.31$, the thrust coefficient, C_T shows a rapid increase as the tip speed ratio increases, λ. A good agreement is obtained between thrust coefficients, C_T of considered wind turbines.

Variation of thrust force, T depending on the tip speed ratio, λ is presented in Fig. 10. The maximum thrust force, T corresponding to 150 kN occurs at the tip speed ratio of λ=5.21. Fig. 11 indicates the relationship between tangential flow induction factor, a' and the tip speed ratio, λ. Tangential flow induction factor, a' for all turbines takes a maximum value of 0.0027 at the tip speed ratios, λ of 5.21. At this condition, a related free-stream wind speed, U_∞ and a hub-height wind speed, U_D are calculated to be 13.35 m/s and 12.36 m/s, respectively.

4. Conclusions

Wind turbine aerodynamic characteristics are quite important in the development of wind turbine technology. Present study involves proper explanations of turbine aerodynamic parameters. Also, among the analyzed data of five turbines, well agreement is reached between each turbine data in terms of aerodynamic parameters. The results obtained from the study are summarized as follows:

- A wind turbine can rotate at different rotational speed during the year. However, optimum rotational speed is very important for maximum turbine efficiency. According to the obtained results, during a year, operating percentage of wind turbines at an optimum rotational speed of 16.40 rpm is determined as 45%.
- At very low wind speeds or low rotational speeds which cannot exert enough torque to the wind

turbine blades to force them rotate, in the case of preventive maintenance and fault detection the wind turbine does not generate much power. It is observed that wind turbines do not generate power approximately for one-fourth of a year.

- Initially, power output remains almost constant between the tip speed ratios of 2.81 and 5.0, and then decreases with increasing tip speed ratio. The maximum wind power output of 2000 kW occurs at a tip-speed ratio of 2.81 and a rotational speed of 16.40 rpm.
- According to the present results, wind turbine efficiency rapidly increases with increasing tip speed ratio and then remains approximately constant, or decreases slightly. Maximum wind turbine efficiency is found to be 30%. Optimum tip speed ratio, which turbines operate most efficiently, is calculated to be 7.12.
- Variations of axial flow induction factor and wind turbine efficiency as a function of tip speed ratio have the same tendency. Minimum and maximum flow induction factors are determined as 0.0124 and 0.0924 at λ=2.81 and λ=7.12, respectively.
- Thrust force on the rotor is an important factor for the performance of wind turbines, and it is directly applied to the tower on which the rotor is attached. Firstly, the thrust force rises rapidly with increasing tip speed ratio, and then decays down sharply. Maximum thrust force is computed to be 150 kN at λ=5.21.

Acknowledgments

The authors wish to thank to the office of Scientific Research Projects of Cukurova University for funding this project under Contract No. FDK-2016-7217 and the Sebenova Wind Farm Association for supplying data.

References

Ageze, M.B., Hu, Y. and Wu, H. (2017), “Wind turbine aeroelastic modeling: Basics and cutting edge trends”, *Int. J. Aerosp. Eng.*, **2017**, 5263897.

Ashrafi, Z.N., Ghaderi, M. and Sedaghat, A. (2015), “Parametric study on off-design aerodynamic performance of a horizontal axis wind turbine blade and proposed pitch control”, *Energ. Convers. Manag.*, **93**, 349-356.

Bai, C.J. and Wang, W.C. (2016), “Review of computational and experimental approaches to analysis of aerodynamic performance in horizontal-axis wind turbines (HAWTs)”, *Renew. Sust. Energ. Rev.*, **63**, 506-519.

Bavanish, B. and Thyagarajan, K. (2013), “Optimization of power coefficient on a horizontal axis wind turbine using bem theory”, *Renew. Sust. Energ. Rev.*, **26**, 169-182.

Bilgili, M., Ozbek, A., Sahin, B. and Kahraman, A. (2015), “An overview of renewable electric power capacity and progress in new technologies in the world”, *Renew. Sust. Energ. Rev.*, **49**, 323-334.

Burton, T., Jenkins, N., Sharpe, D. and Bossanyi, E. (2011), Wind Energy Handbook, (2nd Ed., John Wiley and Sons, Ltd.United Kingdom.

Cao, S., Tamura, Y., Kikuchi, N., Saito, M., Nakayama, I. and Matsuzaki, Y. (2009), “Wind characteristics of a strong typhoon”, *J. Wind Eng. Ind. Aerod.*, **97**, 11-21.

Emejeamara, F.C., Tomlin, A.S. and Millward-Hopkins, J.T. (2015), “Urban wind: Characterisation of useful gust and energy capture”, *Renew. Energ.*, **81**, 162-172.

Hansen, M.O.L., Sørensen, J.N., Voutsinas, S., Sørensen, N. and Madsen, H.A. (2006), “State of the art in wind turbine aerodynamics and aeroelasticity”, *Progress Aerosp. Sci.*, **42**, 285-330.

He, Y., Chan, P. and Li, Q. (2013), “Wind characteristics over different terrains”, *J. Wind Eng. Ind. Aerod.*, **20**, 51-69.

Jeon, S., Kim, B. and Huh, J. (2015), “Comparison and verification of wake models in an onshore wind farm considering single wake condition of the 2 MW wind turbine”, *Energy*, **93**, 1769-1777.

Karthikeyan, N., Murugavel, K.K., Kumar, S.A. and Rajakumar, S. (2015), “Review of aerodynamic developments on small horizontal axis wind turbine blade”, *Renew. Sust. Energ. Rev.*, **42**, 801-822.

Khanjari, A., Sarreshtehdari, A. and Mahmoodi, E. (2017), “Modeling of energy and exergy efficiencies of a wind turbine based on the blade element momentum theory under different roughness intensities”, *J. Energ. Resour. Technol.*, **139**, 022005.

Kishinami, K., Taniguchi, H., Suzuki, J., Ibano, H., Kazunou, T. and Turuhami, M. (2005), “Theoretical and experimental study on the aerodynamic characteristics of a horizontal axis wind turbine”, *Energy*, **30**, 2089-2100.

Lanzafame, R. and Messina, M. (2010), “Horizontal axis wind turbine working at maximum power coefficient continuously”, *Renew. Energ.*, **35**, 301-306.

Manwell, J.F., McGowan, J.G. and Rogers, A.L. (2009), *Wind Energy Explained Theory, Design and Application*, (2nd Ed.), John Wiley & Sons, Ltd., United Kingdom.

Mathew, S. (2006), Wind Energy: Fundamentals, Resource Analysis and Economics, Springer-Verlag Berlin Heidelberg, Netherlands.

Ohunakin, O.S. and Akinnawonu, O.O. (2012), “Assessment of wind energy potential and the economics of wind power generation in Jos, Plateau State, Nigeria”, *Energ. Sust. Develop.*, **16**, 78-83.

Pinto, R.L.U.F. and Gonçalves, B.P.F. (2017), “A revised theoretical analysis of aerodynamic optimization of horizontal-axis wind turbines based on BEM theory”, *Renew. Energ.*, ***105***, 625-636.

REGD (2017), Renewable Energy General Directorate; Wind Energy Technical Potential for the Provinces of Turkey. http://www.eie.gov.tr/.

Rodriguez-Hernandez, O., del Río, J.A. and Jaramillo, O.A. (2016), “The importance of mean time in power resource assessment for small wind turbine applications”, *Energ. Sust. Develop.*, **30**, 32-38.

Sedaghat, A., Assad, M.E.H. and Gaith, M. (2014), “Aerodynamics performance of continuously variable speed horizontal axis wind turbine with optimal blades”, *Energy*, **77**, 752-759.

Sun, Z., Chen, J., Shen, W.Z. and Zhu, W.J. (2016), “Improved blade element momentum theory for wind turbine aerodynamic computations”, *Renew. Energ.*, **96**, 824-831.

Tao, T., Wang, H. and Wu, T. (2017), “Comparative study of the wind characteristics of a strong wind event based on stationary and nonstationary models”, *J. Struct. Eng.- ASCE*, **143**(5), 04016230.

Tenguria, N., Mittal, N.D. and Ahmed, S. (2010), “Investigation of blade performance of horizontal axis wind turbine based on blade element momentum theory (BEMT) using NACA

airfoils", *Int. J. Eng. Sci. Technol.*, **2**(12), 25-35.
VESTAS Global Energy Company (2017); V80-2.0 MW Brochure. https://www.vestas.com/.
Wang, H., Wu, T., Tao, T., Li, A. and Kareem, A. (2016), "Measurements and analysis of non-stationary wind characteristics at Sutong Bridge in Typhoon Damrey", *J. Wind Eng. Ind. Aerod.*, **151**, 100-106.
Wekesa, D.W., Wang, C. and Wei, Y. (2016), "Empirical and numerical analysis of small wind turbine aerodynamic performance at a plateau terrain in Kenya", *Renew. Energ.*, **90**, 377-385.
Zidong, X., Hao, W., Teng, W., Tianyou, T. and Jianxiao, M. (2017), "Wind characteristics at Sutong Bridge site using 8-year field measurement data", *Wind Struct.*, **25**(2), 195-214.

CC